Journal of
Mechanical
Science and
Technology

Journal of Mechanical Science and Technology 21 (2007) 1184~1190

Ultrasonic Beam Propagation in Highly Anisotropic Materials Simulated by Multi-Gaussian Beams

Hyunjo Jeong[a,*], Lester W. Schmerr, Jr.[b]

[a]*Division of Mechanical and Automobile Engineering, Wonkwang University, Iksan, Jeonbuk 570-749, Korea*
[b]*Center for Nondestructive Evaluation and Department of Aerospace Engineering, Iowa State University, Ames, IA 50011, USA*

(Manuscript Received October 11, 2006; Revised May 15, 2007; Accepted July 4, 2007)

Abstract

The necessity of nondestructively inspecting fiber-reinforced composites, austenitic steels, and other inherently anisotropic materials has stimulated considerable interest in developing beam models for anisotropic media. The properties of slowness surface play a key role in the beam models based on the paraxial approximation. In this paper, we apply a modular multi-Gaussian beam (MMGB) model to study the effects of material anisotropy on ultrasonic beam profile. It is shown that the anisotropic effects of beam skew and excess beam divergence enter into the MMGB model through parameters defining the slope and curvature of the slowness surface. The overall beam profile is found when the quasilongitudinal (qL) beam propagates in the symmetry plane of a transversely isotropic gr/ep composite. Simulation results are presented to illustrate the effects of these parameters on ultrasonic beam diffraction and beam skew. The MMGB calculations are also checked by comparing the anisotropy factor and beam skew angle with other analytical solutions.

Keywords: Anisotropic materials; MMGB model; Slowness surface; Beam diffraction/skew

1. Introduction

Multi-Gaussian beam (MGB) models can be used to describe the propagation of ultrasonic beams from planar or focused transducers in a variety of testing situations (Schmerr, 2000; Rudolph, 1999; Song et al., 2004; Kim et al., 2004). One of the attractive features of MGB models is that they are numerically very efficient. This is because these models rely on the superposition of a small number (10-15) of Gaussian beams whose properties can be described in analytical terms even after propagation through general anisotropic media and after interactions with multiple curved interfaces. The MGB models also form an important part of more complete ultrasonic measurement models that can simulate the measured response of defects. In these measurement models, the MGB models are used to predict diffraction correction terms which account for the effects of the acoustic wave fields as they travel from the transducer to the defect and back (Kim et al., 2004; Lopez-Sanchez, 2006). As the number of interfaces increases, however, the an-alytical expressions for the amplitude and phase of a Gaussian beam become increasingly complex. Modular multi-Gaussian beam (MMGB) models (Schmerr and Sedov, 2003) have been developed as an alternative approach. The MMGB model provides an efficient formulation for ultrasound propagation because of its modular matrix form after multiple interface interactions. This modular way of expressing the solution is very convenient to generalize for N transmissions/reflections by representing the propagating Gaussian amplitude and phase in terms of the

*Corresponding author. Tel.: +82 63 850 6690, Fax.: +82 63 850 6691
E-mail address: hjjeong@wonkwang.ac.kr

global matrices for the entire set of multiple propagation and transmission/reflection matrices. The MMGB models were used to calculate the ultrasonic beam profiles for a multilayered isotropic medium with interface curvatures (Huang et al., 2005) and for a contact/angle beam testing (Jeong et al., 2005).

The necessity of nondestructively inspecting fiber-reinforced composites, austenitic steels, and other inherently anisotropic materials has stimulated considerable interest in wave propagation in anisotropic media. The properties of slowness surface play a key role in the beam models based on the paraxial approximation. The essential feature of this approximation is a Taylor series expansion of the slowness surface in the vicinity of the propagation direction. The curvature terms of the slowness surface for wave type α can be obtained by expanding the x_3 component of the slowness vector, $\mathbf{s}_\alpha$, (s_3^α) to the second order in the (x_1, x_2, x_3) coordinates in the form:

$$s_3 = s_0 + As_1 + Bs_2 + \left[C - \frac{1}{2s_0}\right](s_1)^2 + Ds_1 s_2 + \left[E - \frac{1}{2s_0}\right](s_2)^2$$

It is well known that the coefficients of the first- and second-order terms in the expansion of the slowness surface govern the beam skew and divergence respectively. The parameters A and B define the rate of change of slowness with propagation direction, and, hence, determine the group velocity and its direction. This effect is often referred to as beam skew. The parameters C, D, and E define the curvatures of slowness surface. As will be seen, these will determine the rate of divergence or convergence of the beam due to diffraction. The fact that the diffraction in an anisotropic material is related to that in an isotropic material by an "anisotropy factor" has been noted by several authors (Newberry and Thompson, 1989; Norris, 1987; Papadakis, 1964; 1966). This factor can be thought of as the equivalent distance needed to be traveled in an isotropic medium to achieve the same diffraction effects that occur when traveling a distance in the anisotropic medium.

In this paper, we briefly describe a highly modular multi-Gaussian beam model that can be efficiently used to simulate the propagation of ultrasonic beams in an anisotropic solid. We illustrate the effects that changes in the slowness surface curvatures have on an ultrasonic transducer beam radiating into an anisotropic solid through the use of the MMGB model, where the field radiated by a transducer is modeled as the superposition of 10 Gaussian beams. Simulation results are presented for a gr/ep composite when the quasilongitudinal (qL) wave propagates in the symmetry plane of this material. In order to check the MMGB prediction for the anisotropy factor, we set the parameters A-E to be zero for the isotropic solid in which the slowness is equivalent to s_0 for the anisotropic case.

2. A modular Gaussian beam model

We will describe the modular Gaussian approach for the contact setup shown in Fig. 1 where a Gaussian beam is radiated at normal incidence through a planar anotropic solid interface. For the geometry of Fig. 1, we will assume that a Gaussian velocity profile is present at the transducer and propagates as a Gaussian beam into the solid. In Fig. 1, $V(0)$ and $\mathbf{M}(0)$ are the known starting amplitude and phase values in the Gaussian at the transducer location.

When the incident Gaussian beam strikes a general anisotropic solid, a quasi L-wave and two quasi S-waves (qS_1, qS_2) will be generated and propagated. In order to describe the transmitted waves in the solid we employ the coordinates (x_1, x_2, x_3). The x_3 coordi-

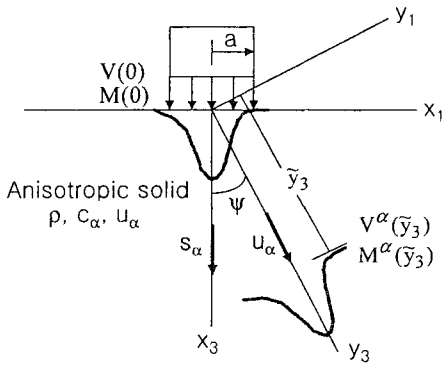

Fig. 1. A Gaussian beam propagation in a general anisotropic solid. Only one of three possible propagating waves is shown. The x_3 coordinate is taken along the direction of the slowness vector, $\mathbf{s}_\alpha$, in the anisotropic solid. For the beam propagation in nonsymmetry directions, y_3 axis is taken along the group velocity direction, $\mathbf{u}_\alpha$, and $y_1 - y_3$ plane is taken as the plane of incidence. The distance $\tilde{y}_3$ is measured along the y_3 axis. The beam skew is measured as an angle between x_3 and y_3 axes.

nate is taken along the direction of the slowness vector in the anisotropic solid and (x_1, x_2) are coordinates orthogonal to the x_3 axis, with x_1 in the plane of incidence and x_2 normal to that plane. The propagation distance $\tilde{x}_3$ is measured in the x_3 direction along the central axis of the Gaussian beam.

When the beam propagates in the nonsymmetry directions, we introduce another coordinates (y_1, y_2, y_3) to describe the beam propagation in terms of the group velocity. The y_3 axis is taken along the group velocity direction and $y_1 - y_3$ plane is taken as the plane of incidence. The distance $\tilde{y}_3$ is measured along the y_3 axis. The beam skew is measured as an angle between x_3 and y_3 axes. For the case of beam propagation in the symmetry directions, the two coordinate systems coincide.

2.1 Gaussian beam propagation in an anisotropic solid

The velocity amplitude $V^{\alpha}(\tilde{y}_3)$ and phase $\mathbf{M}^{\alpha}(\tilde{y}_3)$ of a propagating Gaussian beam of the wave type α in the solid at distance $\tilde{y}_3$ can be completely described by solving the paraxial wave equation (Huang, 2005).

$$\mathbf{v}(\tilde{y}_3, \omega) = \frac{V(0)}{\sqrt{\det[A^{P} + B^{P} M(0)]}} \bar{\mathbf{d}} \exp\left(i\omega \left(\frac{\tilde{y}_3}{u_{\alpha}} + \frac{1}{2} Y^{T} \mathbf{M}^{\alpha}(\tilde{y}_3)\, Y \right) \right) \tag{1}$$

where

$$\mathbf{M}^{\alpha}(\tilde{y}_3) = \left[\mathbf{D}^{P}\, \mathbf{M}(0) + \mathbf{C}^{P} \right] \left[\mathbf{B}^{P}\, \mathbf{M}(0) + A^{P} \right]^{-1} \tag{2}$$

In Eq. (1), the propagation matrices ($\mathbf{A}^{P}$, $\mathbf{B}^{P}$, $\mathbf{C}^{P}$, $\mathbf{D}^{P}$) in the solid are given by

$$\mathbf{A}^{P} = \begin{bmatrix} 1 & 0 \\ 0 & 1 \end{bmatrix},$$

$$\mathbf{B}^{P} = \frac{c_{\alpha}}{u_{\alpha}} \begin{bmatrix} (c_{\alpha} - 2C^{\alpha})\tilde{y}_3 & -D^{\alpha}\tilde{y}_3 \\ -D^{\alpha}\tilde{y}_3 & (c_{\alpha} - 2E^{\alpha})\tilde{y}_3 \end{bmatrix},$$

$$\mathbf{C}^{P} = \begin{bmatrix} 0 & 0 \\ 0 & 0 \end{bmatrix}, \qquad \mathbf{D}^{P} = \begin{bmatrix} 1 & 0 \\ 0 & 1 \end{bmatrix} \tag{3}$$

The 2×2 matrix $\mathbf{M}(0)$ is defined in the next section. In Eq. (3) c_{α} and u_{α} are magnitudes of phase and group velocities for a wave of type α for a given propagation direction. The terms $(C^{\alpha}, D^{\alpha}, E^{\alpha})$ represent the slowness surface curvatures (as measured in the slowness coordinates (x_1, x_2, x_3)) along the refracted ray. In the isotropic case $C^{\alpha} = D^{\alpha} = E^{\alpha} = 0$. These curvature terms can be obtained by expanding the x_3 component of the slowness vector, $\mathbf{s}_{\alpha}$, (s_3^{α}) to the second order in the (x_1, x_2, x_3) coordinates in the form (Rudolph, 1999)

$$s_3^{\alpha} = \frac{1}{c_{\alpha}} - \frac{u_I^{\alpha}}{c_{\alpha}} s_I^{\alpha} + K_{IJ}^{\alpha} s_I^{\alpha} s_J^{\alpha} \quad (I, J = 1, 2) \tag{4}$$

where $(u_1^{\alpha}\ u_2^{\alpha})$ are the components of the group velocity vector, u_{α}, along the (y_1, y_2) axes, respectively, for a wave of type α. For an isotropic solid $u_1^{\alpha} = u_2^{\alpha} = 0$. The matrix $\mathbf{K}^{\alpha}$ in Eq. (4) is given by

$$\mathbf{K}^{\alpha} = -\frac{1}{2} \begin{bmatrix} c_{\alpha} - 2C^{\alpha} & -D^{\alpha} \\ -D^{\alpha} & c_{\alpha} - 2E^{\alpha} \end{bmatrix} \tag{5}$$

For some simple type of anisotropic media the curvature terms can be expressed in analytical form. In general, they must be obtained numerically from the values of the slowness surfaces in the neighborhood of the refracted ray.

2.2 Modular multi-Gaussian beam model

Using the approach of Wen and Breazeale (Wen and Breazeale, 1988), by the superposition of 10 Gaussian beams, one can model the corresponding wave field of a circular piston source (of radius a). In this manner, Eq. (1) can be written as

$$\mathbf{v}^{\alpha}(\tilde{y}_3, \omega) = \sum_{n=1}^{10} \frac{V(0)\, A_n\, \bar{\mathbf{d}}^{\alpha}}{\sqrt{\det\left[\mathbf{A}^{G} + \mathbf{B}^{G}\, (\mathbf{M}(0))_n \right]}} \exp\left[i\omega \left(\frac{\tilde{y}_3}{u_{\alpha}} + \frac{1}{2} \mathbf{Y}^{T} \mathbf{M}^{\alpha}(\tilde{y}_3) \mathbf{Y} \right) \right] \tag{6}$$

where $(\mathbf{M}(0))_n = \frac{2\, i\, B_n}{\omega\, a^2} \mathbf{I}$, and A_n and B_n are ten complex constants (Wen and Breazeale, 1988). Equation (6) provides a highly efficient formulation for modeling the wave fields of ultrasonic transducers in very complex testing situations, and will be referred to as the "MMGB" model.

3. Local properties of slowness surface

Equation (3) shows that the group velocity components and slowness surface curvatures are key parameters needed to define the propagation characteristics of a beam in anisotropic solids. We examine the effects of these parameters when the transducer beam propagates directly into the symmetry plane of the anisotropic solid as shown in Fig. 1.

We use a local fitting procedure to extract the slopes and curvatures from numerical values of the slowness surface in the neighborhood of a particular direction. Equation (4) can be rewritten as

$$s_3 = s_0 + As_1 + Bs_2 + \left[C - \frac{1}{2s_0}\right](s_1)^2 + Ds_1s_2 + \left[E - \frac{1}{2s_0}\right](s_2)^2 \quad (7)$$

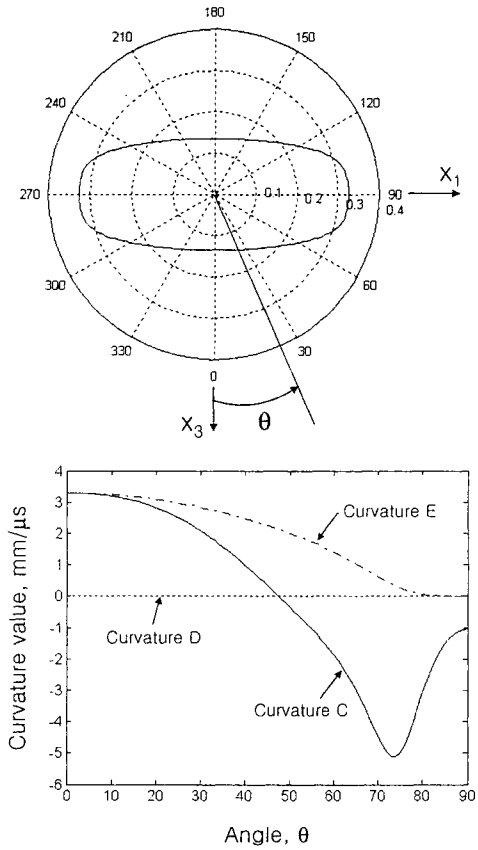

Fig. 2. For the unidirectional gr/ep composite: (a) Slowness curve in $\mu s/mm$ in the $x_1 - x_3$ plane, and (b) Curvatures of qL wave in the $x_1 - x_3$ plane

Sampling a small patch of the slowness surface near the x_3 direction N times will give rise to an $N \times 5$ over-determined system of equations. A least squares method was used to compute the five unknown parameters of the slowness surface.

As an example of the use of this method, we consider the unidirectional gr/ep composite whose properties are assumed to be transversely isotopic: C_{11}=C_{22}=15, C_{12}=7.7, C_{13}=C_{23}=3.4, C_{33}=87, C_{44}=C_{55}= 7.8, C_{66}=3.65 GPa and ρ=1.595 g/cm^3. Figure 2(a) represents the slowness curve of this material as a function of propagation direction in the $x_1 - x_3$ plane. Figure 2(b) plots the curvatures C and E for the qL wave. Note that for this example the parameter D is zero.

4. Results and discussion

Here some results simulated by the MMGB model are presented. The simulation studies show the effects of the slowness curvature changes on the beam propagation. We consider the qL wave radiating directly into the unidirectional composite along the x_3 axis which is along the 0° direction in Fig. 2(a), an axis of symmetry. Under this condition, the slowness parameters for the qL wave are $A^{qL} = B^{qL} = 0$, $C^{qL} = E^{qL} = 3.3\ mm/\mu s$. Since this is an axis of material symmetry, there is no beam skewing ($\Psi = 0$ in Fig. 1 so that y_3 and x_3 axes coincide). Figure 3 shows 2-D beam profiles of the qL wave generated by a 5 MHz, 6.35 mm radius planar transducer. In order to see the effects of the curvature changes on the beam propagation more clearly, we artificially used three different curvature values: C=E=100%, 50%, and 0%. The 0% corresponds to the beam propagation in the isotropic solid with a slowness equivalent to s_0 for the anisotropic case. The profile is computed up to 500 mm in the solid. It is obvious that the beam spreads much slower in the anisotropic case than in the corresponding isotropic case. Shown in Fig. 4 are plots of the on-axis responses corresponding to the beam profiles shown in Fig. 3. It can be clearly seen how the beam profile moves into the transducer face as the curvature of the slowness surface approaches 0. Figure 5 shows the cross-axis beam profiles for three different curvature values at a distance $\tilde{y}_3$ where the on-axis response has its last peak. The last peak is found to occur at $\tilde{y}_3 = 252$ mm and $\tilde{y}_3 = 27$ mm for C=E=100% and 0%, respectively. The cross-axis response (beam width) is unchanged even though the

curvatures of the slowness surface changes significantly. Because the beam width remains the same, the three plots in Fig. 5 are the same and not distinguishable.

The anisotropy factor Λ/λ_z for the qL wave beam radiation into the unidirectional composite along the x_3 axis is given by (Newberry and Thompson, 1989)

$$\frac{\Lambda}{\lambda_z}=\frac{c_{44}}{c_{33}}+\frac{(c_{13}+c_{44})^2}{c_{33}(c_{33}-c_{44})} \tag{8}$$

For an isotropic material, $c_{13}=c_{33}-2c_{44}$, and Λ/λ_z reduces to unity as it should. If we use the elastic constants of the unidirectional composite considered in this study, Eq. (8) yields the anisotropy factor of 0.108. This means that when traveling a distance $\tilde{y}_3$ in the composite the equivalent distance becomes $(\Lambda/\lambda_z)\tilde{y}_3=0.108\tilde{y}_3$ to achieve the same diffraction in an isotropic solid with a slowness equivalent to s_0 of the unidirectional composite. If we refer to Fig. 4, this anisotropy factor is calculated as $27/252\approx 0.107$ from the last peak distances for C=E=100% and 0% cases. Based on these comparisons, the MMGB model seems to provide very accurate diffraction effects.

The MMGB model employed in this paper can be used to determine the transducer beam profile as it propagates in nonsymmetry directions within a symmetry plane. In this case, the anisotropic effects of beam skew and excess beam divergence due to diffraction should be observed at the same time. Due to its highly anisotropic nature, the unidirectional gr/ep composite is expected to show a large amount of beam skew depending on the propagation direction. For this example, the beam profiles are simulated every 10 degrees of propagation angle from the x_3 axis to the x_1 axis.

The simulation results are shown in Fig. 6, where the slowness vector direction (or wave vector direction) in each plot was rotated for illustration purpose so that it indicates vertically downward. Therefore the deviation angle is measured from the vertical axis. Different diffraction effects are observed in each plot since the values of C and E change as a function of propagation angle θ (see Fig. 2b). The beam for $\theta=90^\circ$ pulls more toward the transducer face than the beam for $\theta=0^\circ$. Except for beam propagation in symmetry directions $\theta=0^\circ$ and 90°, the beams for other angles are seen to skew to the left of the inward

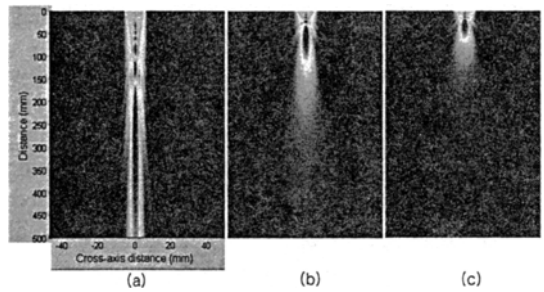

Fig. 3. 2-D beam profiles of a 5 MHz, 6.35 mm diameter planar transducer radiating directly into the unidirectional composite. Slowness curvatures change from C=E=100% to 0%. The 0% corresponds to the isotropic case.

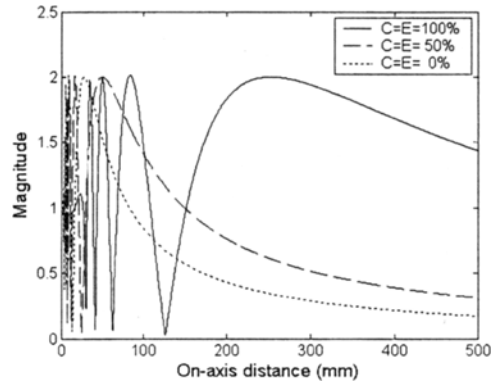

Fig. 4. On-axis responses corresponding to the beam profiles shown in Fig. 3.

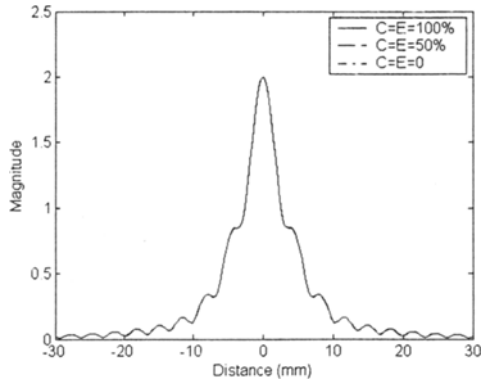

Fig. 5. Cross-axis beam profile at a distance $\tilde{y}_3$ where the on-axis response has its last peak.

normal direction. The approximate skew angle for a given propagation angle can be calculated from $\psi=\arccos\left(1/\sqrt{A^2+B^2+1}\right)$ where A and B are the slopes of the slowness surface, or can be measured directly from the plot in Fig. 6. Figure 7 shows the beam skew

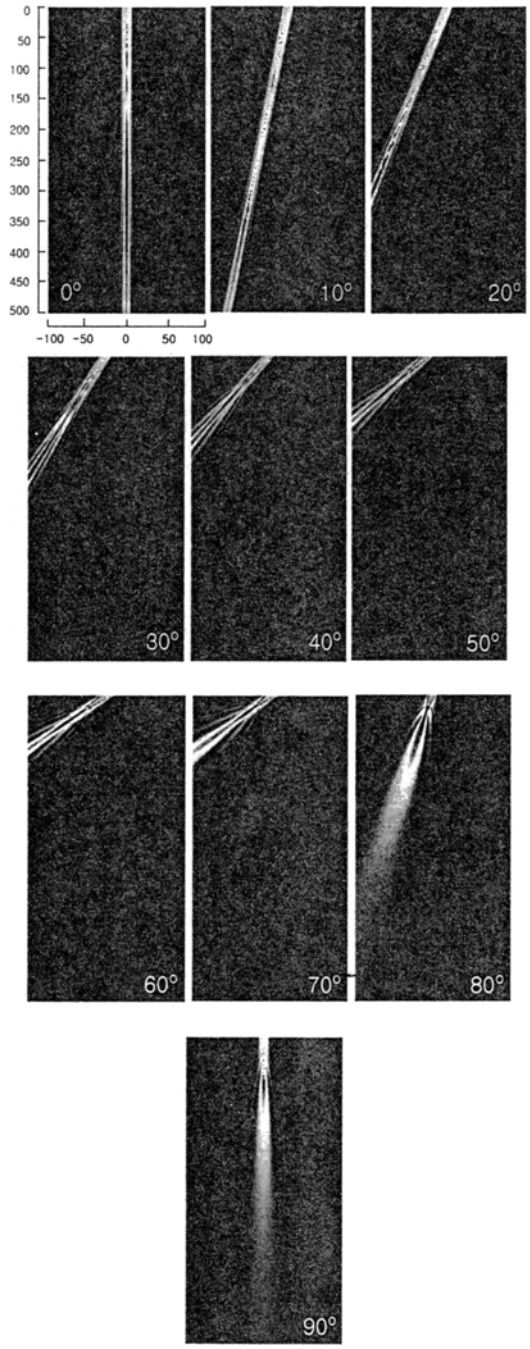

Fig. 6. Beam profiles of a 5 MHz, 6.35 mm diameter planar transducer radiating directly into the unidirectional gr/ep composite.

(deviation) angles obtained from the exact method (Jeong and Park, 2002). It is found from comparisons that the beam model provides correct beam skew angles.

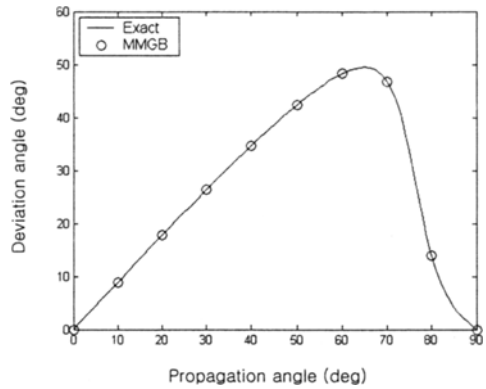

Fig. 7. Beam skew (deviation) angles obtained from the exact method.

Based on these observations, the MMGB model correctly predicts both the beam diffraction and beam skewing due to anisotropy. More complicated effects of the slowness surface are expected when the transducer beam propagates in a more general direction of anisotropic composite materials (i.e., beam propagation in nonsymmetry directions within nonsymmetry planes).

5. Conclusions

The slowness surface parameters such as slopes and curvatures are needed when simulating the beam propagation in anisotropic materials with models based on the paraxial approximation. The slopes of the slowness surface are related to the group velocity components in anisotropic materials, and it is well known that this causes beam skewing. We applied the MMGB model to look at the beam profile in the transversely isotropic unidirectional gr/ep composite. The slowness curvatures also come into the MMGB model. We used a local fitting procedure to extract the curvatures from numerical values of the slowness surface in the neighborhood of a particular direction. Through parametric studies it was shown that the MMGB model correctly predicted the anisotropic effects of beam diffraction and beam skew. Therefore, the MMGB model can be efficiently used to predict the diffraction corrections in ultrasonic measurement models for anisotropic materials.

Acknowledgement

This work was supported by Wonkwang University in the academic year 2005.

Reference

Huang, R., Schmerr, L. W. and Sedov, A., 2005, "Multi-Gaussian Ultrasonic Beam Modeling for Multiple Curved Interfaces – An ABCD Matrix Approach, " *Research in Nondestructive Evaluation*, Vol. 16, pp. 143~174.

Jeong, H. and Park, M. C., 2002, "Finite Element Analysis of Ultrasonic Wave Propagation in Anisotropic Materials," *Journal of the Korean Society for Mechanical Engineers A*, Vol. 26, No. 10, pp. 2201~2210.

Jeong, H., Park, M. C. and Schmerr, L. W., 2005, "Application of a Modular Multi-Gaussian Beam Model to Some NDE Problems, Review of Progress in Quantitative Nondestructive Evaluation," Vol. 24, ed. by D. O. *Thompson and D. E. Chimenti*, pp. 986~993.

Kim, H. J., Song, S. J. and Schmerr, L. W., 2004, "Modeling Ultrasonic Pulse-echo Signals from a Flat-bottom Hole in Immersion Testing Using a Multi-Gaussian Beam," *Journal of Nondestructive Evaluation*, Vol. 23, pp. 11~19.

Kim, H. J., Park, J. S., Song, S. J. and Schmerr, L. W., 2004, "Modeling Angle Beam Ultrasonic Testing Using Multi-Gaussian Beams," *Journal of Nondestructive Evaluation*, Vol. 23, pp. 81~93.

Lopez-Sanchez, A. L, Kim, H. J., Schmerr, L. W. and Gray, T. A., 2006, "Modeling the Response of Ultrasonic Reference Reflectors," *Research in Nondestructive Evaluation*, Vol. 17, pp. 49~69.

Newberry, B. P. and Thompson, R. B., 1989, "A Paraxial Theory for the Propagation of Ultrasonic Beams in Anisotropic Solids," *J. Acoust. Soc. Am.*, Vol. 85, pp. 2290~2300.

Norris, A. N., 1987, "A Theory of Pulse Propagation in Anisotropic Elastic Solids," *Wave Motion*, Vol. 9, pp. 1~24.

Ogilvy, J. A., 1986, "Ultrasonic Beam Profiles and Beam Propagation in an Austenitic Weld Using a Theoretical Ray Tracing Model, Ultrasonics," Vol. 24, pp. 337~347.

Papadakis, E. P., 1964, "Diffraction of Ultrasound Radiating into an Elastically Anisotropic Medium," *J. Acoust. Soc. Am.*, Vol. 36, pp. 414~422.

Papadakis, E. P., 1966, "Ultrasonic Diffraction Loss and Phase Change in Anisotropic Materials," *J. Acoust. Soc. Am.*, Vol. 40, pp. 863~876.

Rudolph, M., 1999, "Ultrasonic Beam Models in Anisotropic Media," Ph.D. Thesis, Iowa State University.

Schmerr, L. W. and Sedov, A., 2003, "A Modular Multi-Gaussian Beam Model for Isotropic and Anisotropic Media," *Review of Progress in Quantitative Nondestructive Evaluation*, Vol. 24, ed. by D. O. Thompson and D. E. Chimenti, pp. 828~835.

Schmerr, L. W., 2000, "A Multi-Gaussian Ultrasonic Beam Model for High Performance Simulations on a Personal Computer," *Materials Evaluation*, Vol. 58, pp. 882~888.

Song, S. J., Park, J. S., Kim, Y. H., Jeong, H. and Choi, Y.-H., 2004, "Prediction of Angle Beam Ultrasonic Testing Signals from a Surface Breaking Crack in a Plate Using Multi-Gaussian Beams and Ray Methods," *Review of Progress in Quantitative Nondestructive Evaluation*, Vol. 23, ed. by D. O. Thompson and D. E. Chimenti, pp. 110~117.

Szabo, T. L. and Slobodnik, A. J., 1973, "The Effect of Diffraction on the Design of Acoustic Surface Wave Devices," *IEEE Trans. Sonics Ultrason.*, SU20, pp. 240~251.

Wen, J. J. and Breazeale, M. A., 1988, "A Diffraction Beam Field Expressed as the Superposition of Gaussian Beams," *J. Acoustic. Soc. Am.*, Vol. 83, No. 5, 1752~1756.